Optical Engineering

OpticalEngineering.SPIEDigitalLibrary.org

Spectroscopic study of terahertz reflection and transmission properties of carbon-fiber-reinforced plastic composites

Jin Zhang
Changcheng Shi
Yuting Ma
Xiaohui Han
Wei Li
Tianying Chang
Dongshan Wei
Chunlei Du
Hong-Liang Cui

SPIE.

Spectroscopic study of terahertz reflection and transmission properties of carbon-fiber-reinforced plastic composites

Jin Zhang,[a] Changcheng Shi,[b] Yuting Ma,[a] Xiaohui Han,[a] Wei Li,[b] Tianying Chang,[a,b] Dongshan Wei,[b] Chunlei Du,[b] and Hong-Liang Cui[a,b,*]

[a]Jilin University, College of Instrumentation and Electrical Engineering, Changchun 130061, China
[b]Chinese Academy of Sciences, Research Center for Terahertz Technology, Chongqing Institute of Green and Intelligent Technology, Key Laboratory of Multi-scale Manufacturing Technology, Chongqing 400714, China

Abstract. Carbon-fiber-reinforced plastic (CFRP) composites are widely used in aerospace and concrete structure reinforcement due to their high strength and light weight. Terahertz (THz) time-domain spectroscopy is an attractive tool for defect inspection in CFRP composites. In order to improve THz nondestructive testing of CFRP composites, we have carried out systematic investigations of THz reflection and transmission properties of CFRP. Unidirectional CFRP composites with different thicknesses are measured with polarization directions 0 deg to 90 deg with respect to the fiber direction, in both reflection and transmission modes. As shown in the experiments, CFRP composites are electrically conducting and therefore exhibit a high THz reflectivity. In addition, CFRP composites have polarization-dependent reflectivity and transmissivity for THz radiation. The reflected THz power in the case of parallel polarization is nearly 1.8 times higher than for perpendicular polarization. At the same time, in the transmission of THz wave, a CFRP acts as a Fabry–Pérot cavity resulting from multiple internal reflections from the CFRP–air interfaces. Moreover, from the measured data, we extract the refractive index and absorption coefficient of CFRP composites in the THz frequency range. [DOI: 10.1117/1.OE.54.5.054106]

Keywords: carbon-fiber-reinforced plastic; terahertz; reflection; transmission; refractive index; Fabry–Pérot cavity.

Paper 150056 received Jan. 13, 2015; accepted for publication Apr. 30, 2015; published online May 21, 2015.

1 Introduction

The terahertz (THz) region lies between the microwave and infrared zones of the electromagnetic spectrum, with the frequency ranging from 0.1 to 10 THz.[1,2] In the past two decades, THz science and technology have been developed tremendously due to impressive improvements of ultrafast optoelectronics and low-dimensional semiconductor technology. The applications of THz technology have been extended to security,[3] pharmaceutical sciences,[4] nondestructive evaluation (NDE),[5,6] and many others. Carbon-fiber-reinforced plastic (CFRP) laminates are useful composite materials. Because of their high stiffness and strength, they are commonly used wherever a high strength-to-weight ratio and rigidity are required such as in aerospace, automotive, civil engineering, sporting goods, and so on. The wide utilization of CFRP composites calls for correspondingly advanced methods and technologies for detecting their defects and flaws, especially in NDE.[7,8] The current standard NDE technologies for CFRP are ultrasonic-based[9] and x-ray-based[10,11] testing and imaging methods, which have advantages and limitations. For instance, close contact with a test sample is required for ultrasonic testing, and harmful radiation must be involved in x-ray methods.

In recent years, THz technology has received increasing interest and attention as a potential NDE method for CFRP due to its unique features such as penetrability with respect to nonpolar materials, low-photon-energy radiation, and spectroscopic fingerprinting ability.[12–14] Many studies have been reported regarding NDE for CFRP by using THz technologies. Redo-Sanchez and Karpowicz[15] and Karpowicz and Dawes[16] applied THz continuous and pulsed wave technology in reflection mode to detect burn damage of CFRP. Im et al.[17,18] and Park and Im[19] investigated the electrical field characterization in conducting carbon fiber. Additionally, a reflective THz time-domain spectroscopy (TDS) system was utilized to evaluate polyphenylene sulfide CFRP solid laminate with different angles of orientation of the carbon fibers. The THz scanning images showed the fiber orientation information therein and predicted the orientation of the ply. Yang et al.[20] detected the impact damages in CFRP specimens using millimeter waves of 65 to 67 GHz. When the electric field vector direction is parallel to the carbon fiber direction, reflection coefficients on the surface with and without damage were easily distinguished and damage detection is possible. Ospald et al.[21] analyzed misprocessed coating layers on CFRP panels with high depth resolution. The coating misprocesses can be detected through changes in the propagation time of the reflected THz pulses that are induced by the different dielectric layers.

In the previous studies, the THz reflection properties of CFRP have been fully characterized. However, to our knowledge, there are few studies on the THz transmission properties of CFRP, especially for thin layers of CFRP. In this paper, THz reflection and transmission properties of unidirectional CFRP composites with different thicknesses (e.g., 140 to 550 μm) are investigated systematically. It is found that the reflectivity and transmissivity of CFRP for THz

*Address all correspondence to: Hong-Liang Cui, E-mail: hcui@jlu.edu.cn

radiation depend on the angle between the fiber direction and electric field direction. When the fiber direction is parallel to the electric field direction, the THz reflected power of CFRP is fairly close to that of an aluminum metal plate while the transmitted power is relatively low. When the fiber direction is perpendicular to the electric field direction, the THz reflected power of CFRP is about half of that from the aluminum metal plate while the transmitted power is the highest compared with other angles. When compared among different thicknesses in the through-transmission mode, CFRP composites exhibit an abnormal phenomenon in that the transmitted power of a 2-ply CFRP is distinctly greater than that of a 1-ply CFRP from 0.1 to 0.2 THz. The underlying reason is that the CFRP acts as a Fabry–Pérot cavity and the transmitted power is strengthened at the resonant frequency. Furthermore, the refractive index and absorption coefficient of CFRP composites are obtained in this paper.

The remainder of this paper is organized as follows. First, we describe the related theories about refractive index and electric field characterization of CFRP in Sec. 2. Section 3 introduces the CFRP samples used in our experiments. Next, we explain the THz TDS system from which data are presented in Sec. 4. The experimental results and discussion are given in Sec. 5. Finally, concluding remarks and a summary are presented in the last section.

2 Theoretical Background

2.1 *Refractive Index and Absorption Coefficient*

In analyzing the refractive index, two approaches are employed in the through-transmission mode. The first one was used to calculate the time delay based on the optical path length difference and can be solved by Eq. (1):[17–19]

$$n_s = 1 + \frac{\Delta t V_{\text{air}}}{d}, \tag{1}$$

where d is the sample thickness, V_{air} is the THz wave propagation speed in the air, and Δt is the propagation time difference with and without the sample. In the second approach, the frequency-dependent complex refractive index of the sample is calculated by minimizing the difference between the measured and the theoretical transfer functions. The complex refractive index can be expressed as: $\tilde{n}(\omega) = n(\omega) - i\kappa(\omega)$, where $n(\omega)$ represents the real refractive index, $\kappa(\omega)$ is the extinction coefficient, which is proportional to the absorption coefficient, and ω is the angular frequency. Further information about the specific algorithm employed in this paper is in Ref. 22.

2.2 *Electric Field Characterization of Carbon-Fiber-Reinforced Plastic*

In a unidirectional CFRP, the relationship between the electrical conductivity of CFRP and fiber direction can be expressed as follows:[23]

$$\sigma(\theta) = \sigma_l \cos^2\theta + \sigma_t \sin^2\theta, \tag{2}$$

where $\sigma(\theta)$ is the overall electrical conductivity at θ, and θ is the angle between the fiber direction and electric field direction. σ_l and σ_t are the longitudinal and transverse conductivities, respectively. Since σ_l is much greater than σ_t, Eq. (2) may be written as follows:

$$\sigma(\theta) \approx \sigma_l \cos^2\theta. \tag{3}$$

Consequently, the reflectivity of CFRP may be described as[15,16]

$$R = R_C \cos^2\theta + R_b, \tag{4}$$

where R_C describes the polarization-sensitive reflectivity of carbon fibers, and R_b describes the reflectivity of the background (the epoxy matrix).

3 Preparation of the CFRP Samples

In this study, unidirectional CFRP samples with different numbers of plies are prepared for investigation with pulsed THz radiation. These samples are 1-, 2-, 3-, and 4-ply, with corresponding thickness of 0.14, 0.31, 0.42, and 0.55 mm. All the samples used in our experiments consist of two parts: carbon fiber (67% volume) and epoxy resin (33% volume). The former gives CFRP its strength and rigidity, and the latter binds the carbon fibers together. In addition, the orientations of the carbon fibers in our samples are all the same. Figure 1 shows the optical images of the samples, clearly showing that the fibers' orientation is unidirectional.

4 THz Time-Domain Spectroscopy

A commercially available THz TDS system T-Gauge 5000 from Advanced Photonix, Inc. is employed in this research.[24] Figure 2 shows a schematic diagram of the THz TDS system in the through-transmission and reflection mode. The THz TDS system begins with a Ti:Sapphire oscillator, which

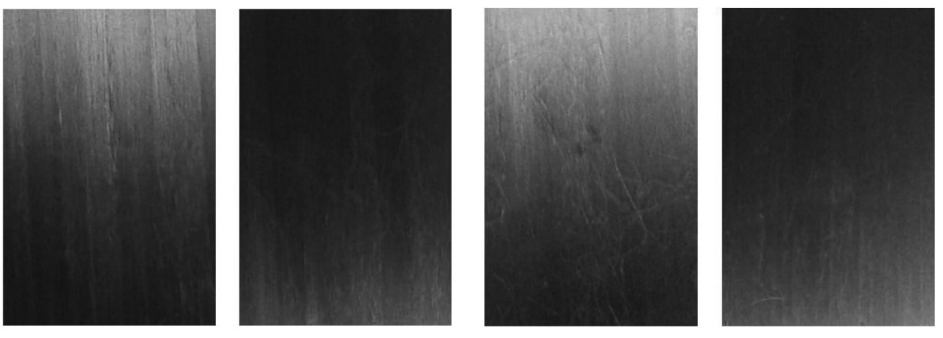

Fig. 1 The optical images of samples: (a) 1-ply, (b) 2-ply, (c) 3-ply, and (d) 4-ply.

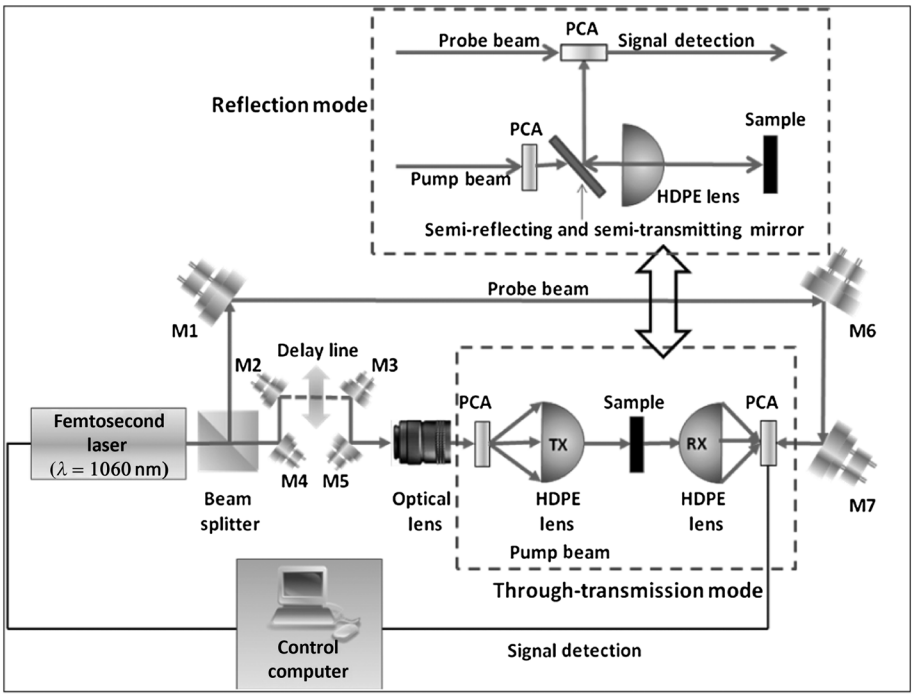

Fig. 2 Schematic diagram of the THz TDS system in the through-transmission and reflection modes (M1–M7: mirrors; HDPE: high-density polyethylene; PCA: photoconductive antenna; TX: transmitter; and RX: receiver).

produces pulses of 1064 nm central wavelength, 80 fs duration, and 100 MHz repetition rate, with an average power of 20 mW. In the through-transmission mode, the transmitter and receiver are mounted on the spectroscopy rail to perform transmission spectroscopic measurements. In the reflection mode, the transmitter and receiver are coupled with the collinear adapter to perform as a collinear reflection transceiver. Due to the restriction of this unique THz TDS system configuration, it is not possible to perform simultaneous THz transmission and reflection measurements of the spectroscopic properties of CFRP samples. The main specifications/parameters of the system are as follows: a spectral range of 0.1 to 3.5 THz with a spectral resolution of 12.5 GHz, a signal-to-noise ratio of better than 70 dB at the lower frequency end, and about 30 dB at the high-frequency end, a time-domain range of 0 to 80 ps with 0.1 ps resolution, and a rapid scanning rate of 1 kHz.

5 Experimental Results and Discussion

5.1 *Results Obtained in the Reflection Mode*

As the CFRP is highly anisotropic, the reflected power from the 1-ply CFRP exhibits a strong angular dependence as expected. The measurements were carried out at every 15 deg angle in our experiments. The angle of 0 deg represents the case that the fiber direction is parallel with the electric field direction (parallel polarization), whereas 90 deg corresponds to the case that the fiber direction is orthogonal to the electric field direction (perpendicular polarization). The total spectrointegrated reflected powers at different angles with a frequency range from 0.1 to 1 THz are calculated and are shown as the seven data points in Fig. 3. As can be seen from Fig. 3, the reflected power decreases as the angle increases from 0 to 90 deg. The seven points are fitted to the relation represented by Eq. (4), and the black curve in Fig. 3 is the final fitting curve. The fit result is $R = 130.93 * \cos^2\theta + 169.8$ and the goodness-of-fit statistics is 99.67%. Through the high goodness of the fit, it is again verified experimentally that the reflectivity of CFRP indeed satisfies Eq. (4).

In our experiments, we compared the total reflected power from the 1-ply CFRP with that from a reference aluminum plate. The spectrointegrated reflected power from 0.1 to 1 THz of CFRP in the case of parallel polarization is 94.5%, relative to that of the reference, whereas it is 53.6% in the case of perpendicular polarization.

Based on the aforementioned observations, we have carried out a preliminary test of the THz reflection

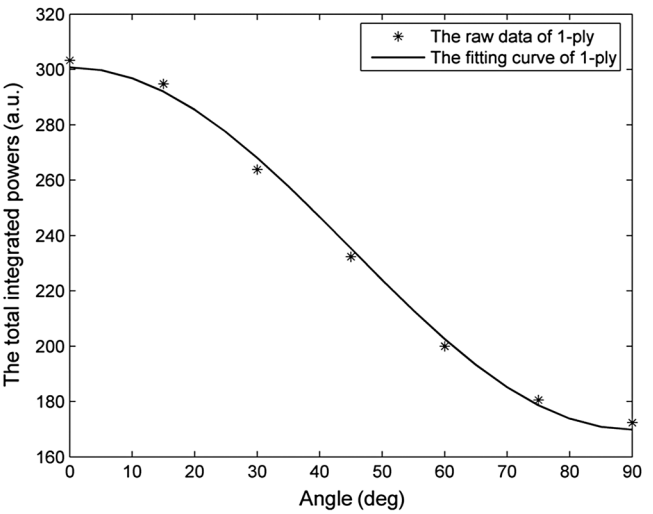

Fig. 3 Angular dependence of reflected power through 1-ply carbon-fiber-reinforced plastic (CFRP).

spectroscopic setup for imaging of a buried defect in the CFRP. The reflective imaging results of a CFRP sample with a Teflon artificial insert are shown in Fig. 4. The Teflon sheet ($50 \times 10 \times 0.2$ mm) was deliberately inserted between two single-ply unidirectional CFRP sheets ($100 \times 100 \times 0.14$ mm) through a hot-press process to simulate a foreign inclusion and/or an inter-ply delaminational defect. In the case of parallel polarization, the incident THz power is almost fully reflected by the first ply CFRP and the hidden defect cannot be detected, as seen in Fig. 4(b). THz waves can penetrate deeper into the CFRP composite and access more depth-related information for perpendicular polarization, such that the defect is readily visualized in Fig. 4(c) without any graphical filtering. After a simple textbook linear-contrast-enhancement processing of the image, the defect becomes much clearer, as shown in Fig. 4(d), which shows basically a diffraction-limited rendition of the hidden defect.

To fully realize the potential of THz imaging techniques in NDE/NDI of composite materials, it is obvious that much more effort needs to be conducted. At present, we are mainly focusing on thin-film coatings on CFRP composites and sandwiched structures involving thin layers of CFRP and dielectrics. The polarization direction of the THz radiation plays an important role in such THz imaging techniques of CFRP related composites, as demonstrated quite convincingly in Fig. 4.

5.2 *Results Obtained in the Through-Transmission Mode*

Figure 5 shows the power transmission ratios of 1-ply CFRP measured at every 15 deg angle (the power spectrum after

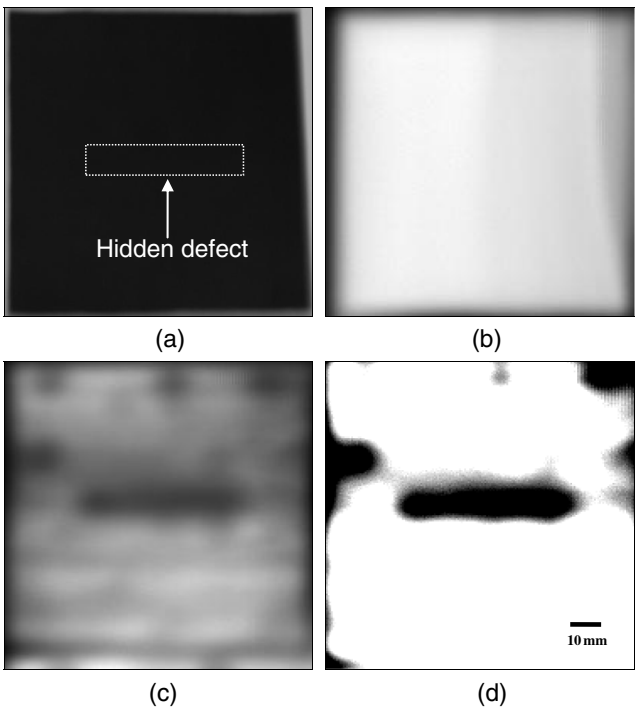

Fig. 4 The reflective imaging results of a Teflon artificial insert defect: (a) front side optical image, (b) THz power image in the parallel polarization mode at 0.075 THz, (c) THz power image in the perpendicular polarization mode at 0.075 THz, and (d) the result after a simple image enhancement process.

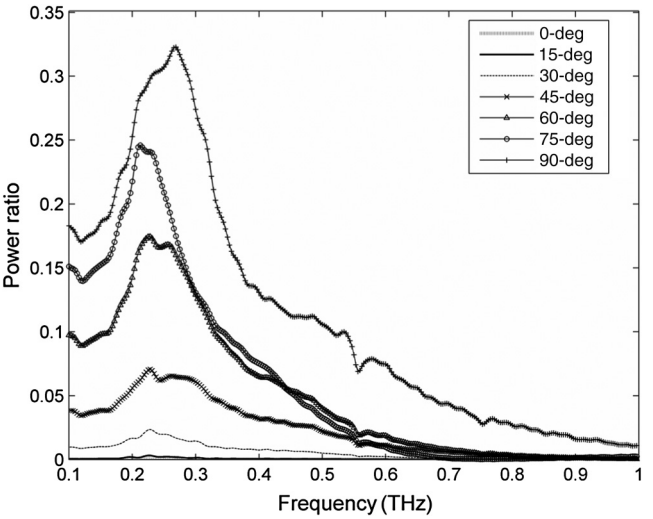

Fig. 5 The power transmission ratio of 1-ply CFRP at different angles.

propagation through the CFRP sample divided by the power spectrum for the air). As can be seen from Fig. 5, THz waves can penetrate the most when the fiber direction is orthogonal with the electric field direction.

The refractive index of CFRP with different angles and thicknesses calculated through the first approach is shown in Table 1. The formula to calculate the resolution of refractive index can be obtained through a derivative operation on Eq. (1), leading to

$$\Delta_{n_s} = \frac{V_{\text{air}}}{d} * \Delta_t. \tag{5}$$

The resolution of time delay in our system is 0.1 ps. According to Eq. (5), we estimate that the resolution of refractive index is 0.2143, 0.0968, 0.0714, and 0.0545 for 1-ply, 2-ply, 3-ply, and 4-ply, respectively. From Table 1, we see that the standard deviations of the measured refractive index are smaller than the theoretical resolution. Hence, we can conclude that within our measurement error, the refractive index of CFRP is a scalar quantity and does not depend on the fiber direction (the electrical conductivity of CFRP). As can be seen from Table 1, there are some variations in the refractive index for CFRP with different thicknesses. That is because CFRP samples are composite materials and the composition of carbon fiber and epoxy resin for CFRP with different thicknesses may vary slightly.

The frequency-dependent refractive index and absorption coefficient of 4-ply CFRP at different angles calculated through the second approach are separately shown in Figs. 6 and 7. We can see that the refractive index of 4-ply CFRP obtained by the second approach is basically consistent with the first approach, and similarly have no direct relationship with the angle between the fiber direction and electric field direction. Over the entire frequency range, the absorption coefficient gradually increases with frequency. In addition, it decreases as the angle increases from 15 to 90 deg. The increase of the angle from 15 to 90 deg entails the decrease of the electrical conductivity of CFRP (see our previous discussion). In other words, the absorption coefficient decreases with the electrical conductivity of CFRP, which agrees with the common

Table 1 The terahertz (THz) refractive index of carbon-fiber-reinforced plastic (CFRP).

Samples	Angle (deg)						Mean ± STD
	90	75	60	45	30	15	
1-ply	4.1957	4.3955	4.3955	4.1957	4.3955	4.5952	4.3622 ± 0.1504
2-ply	4.1389	4.0438	4.1389	3.9486	3.9486	4.0438	4.0438 ± 0.0851
3-ply	4.6466	4.5764	4.5764	4.5063	4.5764	4.5764	4.5764 ± 0.0444
4-ply	4.8376	4.9488	4.8932	4.8376	4.8376	4.8376	4.8654 ± 0.0465

knowledge that the absorption coefficient is proportional to the electrical conductivity.[25] Because the transmitted power of CFRP at 0 deg angle is relatively low, the THz pulse of CFRP is submerged in the noise, and as a result we can obtain accurate optical parameters with neither approach.

Figure 8 is the power transmission ratios of CFRP with different thicknesses at a 90 deg angle. Generally speaking, the transmitted power decreases with the increase of sample thickness. However, there is an interesting anomaly in the frequency range from 0.1 to 0.2 THz in Fig. 8. The transmitted power of the 2-ply CFRP is significantly greater than that of the 1-ply CFRP. This is because that the CFRP acts as Fabry–Pérot cavity for the THz wave and all the resonant frequencies are quite obvious.[26] The optical path difference of two adjacent transmitted THz waves is given as

$$D = 2nh\cos\alpha, \tag{6}$$

where n is the refractive index of the sample, h is the sample thickness, and α is the incident angle. When $D = k\lambda$ $(k = 1, 2, 3\ldots)$, the phases of all the transmitted THz waves are the same and the transmitted power is constructively strengthened.

When THz wave is vertically incident, we can derive the resonant frequencies from the equation $D = 2nh = k\lambda$ $(k = 1, 2, 3\ldots)$

$$f_k = k\frac{c}{2nh}, \quad \text{for } k = 1, 2, 3, \ldots. \tag{7}$$

This formula can predict all the peak positions where the transmitted power is strengthened. Table 2 gives the comparison between measured and calculated peak positions

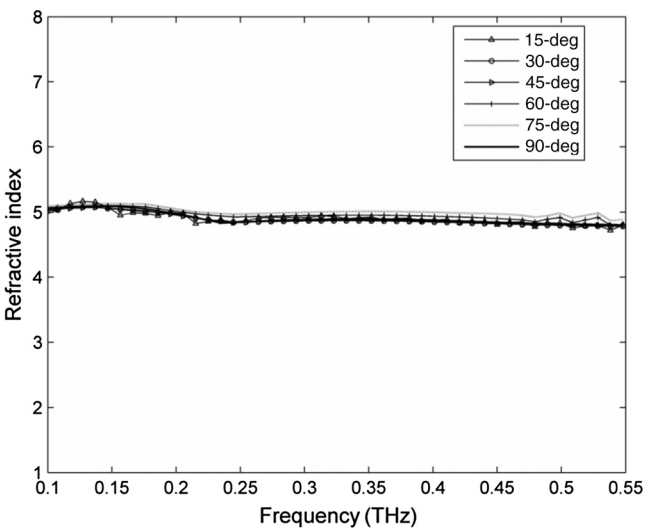

Fig. 6 The refractive index of 4-ply CFRP at different angles.

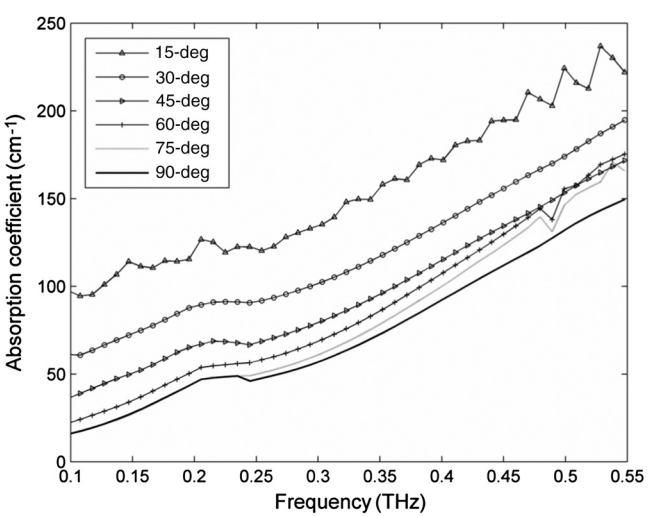

Fig. 7 The absorption coefficient of 4-ply CFRP at different angles.

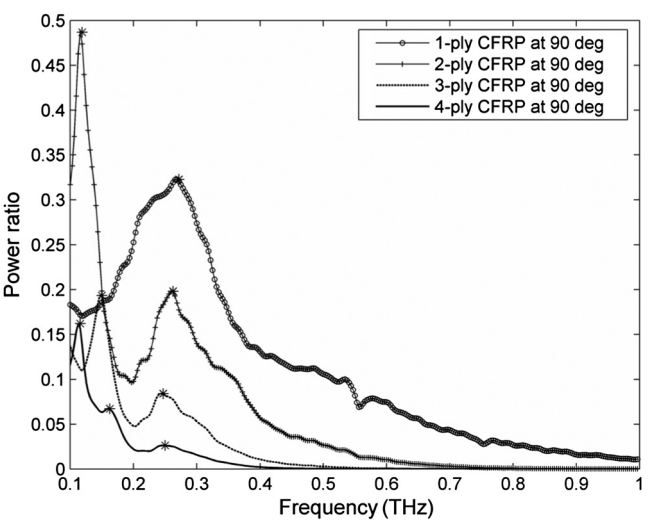

Fig. 8 The power transmission ratio of CFRP with different thicknesses.

Table 2 The comparison between measured and calculated peak positions.

Samples	Refractive index	Thickness (mm)	K	Calculated resonant frequencies (THz)	Measured resonant frequencies (THz)	Relative error (%)
1-ply	4.1957	0.14	1	0.2551	0.2719	6.5857
2-ply	4.1389	0.31	1	0.1169	0.1189	1.7109
2-ply	4.1389	0.31	2	0.2338	0.2625	12.2754
3-ply	4.6466	0.42	2	0.1536	0.1500	2.3438
3-ply	4.6466	0.42	3	0.2304	0.2469	7.1615
4-ply	4.8376	0.55	2	0.1127	0.1156	2.5732
4-ply	4.8376	0.55	3	0.1690	0.1625	3.8462
4-ply	4.8376	0.55	4	0.2254	0.2500	10.9139

and we can see that the measured peak positions have a good agreement with those of the calculated values.

The transmitted THz power of CFRP at different frequencies is determined by both sample thickness and the Fabry–Perót effect. From 0.1 to 0.2 THz, the Fabry–Perót effect may play a major role, so when the resonant peaks occur, the transmitted THz power of a thicker CFRP could be larger than that of thinner CFRP within certain frequency ranges (e.g., 2-ply > 1-ply and 4-ply > 3ply). When the frequency exceeds 0.2 THz, the thickness of the samples starts to become a leading factor, so the transmitted power decreases monotonously when the sample thickness increases.

6 Conclusion

In conclusion, we have conducted a systematic investigation of THz reflection and transmission properties of unidirectional CFRP composites with thin-layer structures (i.e., 1- to 4-ply). Due to the strong anisotropy resulting from fiber orientation, the THz reflection and transmission properties of the CFRP samples are orientation-dependent. The THz reflection power reaches the highest value when the fiber direction is parallel to the THz electric field orientation and the lowest value under the condition of perpendicular polarization. These results are in good agreement with previous studies.[15–19] Concomitantly, the THz transmission power increases when the angle between the fiber and electric field directions increases from 0 deg to 90 deg, which has not been convincingly demonstrated to date. Furthermore, the optical parameters (e.g., refractive index and absorption coefficient) of CFRP composites are obtained in this paper. Interestingly, and perhaps technologically of importance, we found Fabry–Perót echoes in the transmitted power spectra, resulting from multiple internal reflections from the CFRP–air interfaces. Our investigation has achieved some interesting and useful results, but there are still limitations that must be overcome in the future. Based on this study, we note that CFRP composites have a prominent polarizing effect on THz waves and, as such, can be used to fabricate low-cost, flexible, and easy-to-use THz-polarization devices. Furthermore, the conductivity of CFRP hinders the penetration of THz wave into the samples, rendering it difficult to use THz technology to detect internal flaws of CFRP samples with over 1 mm thickness. On the other hand, it would be more advantageous to focus on research pertinent to thickness and defect inspection of dielectric and ceramic coatings on the surface of CFRPs, and thin CFRP–dielectric sandwiched structures in the reflection modality of THz imaging technology, for which the present study may serve as a precursor, and as such, it lays the foundation for future work along this direction.

Acknowledgments

This work is supported by the National Science & Technology Pillar Program during the 12th Five-year Plan Period (2012BAK04B03), the application and development project in Chongqing Science and Technology Commission (cstc2013yykfC00007), and the West Light Foundation of the Chinese Academy of Sciences.

References

1. C. Sirtori, "Bridge for the terahertz gap," *Nature* **417**(6885), 132–133 (2002).
2. R. Won, "NPO 2010 bridging the terahertz gap," *Nat. Photonics* **4**(10), 673–674 (2010).
3. J. F. Federici et al., "THz imaging and sensing for security applications —explosives, weapons and drugs," *Semicond. Sci. Technol.* **20**(7), 266–280 (2005).
4. K. E. Peiponen et al., "Broadening of a THz pulse as a measure of the porosity of pharmaceutical tablets," *Int. J. Pharm.* **447**(1–2), 7–11 (2013).
5. N. Palka and D. Miedzinska, "Detailed non-destructive evaluation of UHMWPE composites in the terahertz range," *Opt. Quantum Electron.* **46**(4), 515–525 (2014).
6. K. Kawase and T. Shibuya, "THz imaging techniques for nondestructive inspections," *C. R. Phys.* **11**(7–8), 510–518 (2010).
7. M. V. Hosur and C. R. L. Murthy, "Estimation of impact-induced damage in CFRP laminates through ultrasonic imaging," *NDT&E Int.* **31**, 359–374 (1998).
8. H. Tsuda, "Ultrasound and damage detection in CFRP using fiber Bragg grating sensors," *Compos. Sci. Technol.* **66**, 676–683 (2006).
9. A. Osman et al., "Automated segmentation of ultrasonic volumetric data of composite materials," *Insight Non-Destr. Test. Cond. Monit.* **57**(3), 153–160 (2015).
10. P. J. Schilling et al., "X-ray computed microtomography of internal damage in fiber reinforced polymer matrix composites," *Compos. Sci. Technol.* **65**, 2071–2078 (2005).
11. F. Sket et al., "Automatic quantification of matrix cracking and fiber rotation by X-ray computed tomography in shear-deformed carbon fiber-reinforced laminates," *Compos. Sci. Technol.* **90**, 129–138 (2014).
12. J. A. Hejase et al., "Terahertz characterization of dielectric substrates for component design and nondestructive evaluation of packages," *IEEE Trans. Comp., Packag., Manuf. Technol.* **1**(11), 1685–1694 (2011).

13. C. Stoik, M. Bohn, and J. Blackshire, "Nondestructive evaluation of aircraft composites using reflective terahertz time domain spectroscopy," *NDT&E Int.* **43**(2), 106–115 (2010).
14. E. Cristofani et al., "Nondestructive testing potential evaluation of a terahertz frequency-modulated continuous-wave imager for composite materials inspection," *Opt. Eng.* **53**(3), 031211 (2014).
15. A. Redo Sanchez and N. Karpowicz, "Damage and defect inspection with terahertz waves," in *The 4th Int. Workshop on Ultrasonic and Advanced Methods for Nondestructive Testing and Material Characterization*, pp. 67–78 (2006).
16. N. Karpowicz and D. Dawes, "Fire damage on carbon fiber materials characterized by THz waves," *Int. J. High Speed Electron. Syst.* **17**(02), 213–224 (2007).
17. K. H. Im and D. K. Hsu, "Terahertz radiation study on FRP composite solid laminates," *AIP Conf. Proc.* **1430**, 1192–1199 (2012).
18. K. H. Im et al., "Influence of terahertz waves on unidirectional carbon fibers in CFRP composite materials," *Mater. Sci.-Medzg.* **20**(4), 457–463 (2014).
19. J. W. Park and K. H. Im, "Terahertz spectroscopy approach of the fiber orientation influence on CFRP composite solid laminates," *J. Mech. Sci. Technol.* **26**(7), 2051–2054 (2012).
20. S. H. Yang and K. B. Kim, "Non-contact detection of impact damage in CFRP composites using millimeter-wave reflection and considering carbon fiber direction," *NDT&E Int.* **57**, 49–51 (2013).
21. F. Ospald et al., "Aeronautics composite material inspection with a terahertz time-domain spectroscopy system," *Opt. Eng.* **53**(3), 1–14 (2014).
22. M. Scheller, C. Jansen, and M. Koch, "Analyzing sub-100-μm samples with transmission terahertz time domain spectroscopy," *Opt. Commun.* **282**(7), 1304–1306 (2009).
23. K. W. Tse, C. A. Moyer, and S. Arajs, "Electrical conductivity of graphite fiber-epoxy resin composites," *Mater. Sci. Eng.* **49**, 41–46 (1981).
24. J. Labaune et al., "Papyrus imaging with terahertz time domain spectroscopy," *Appl. Phys. A-Mater.* **100**(3), 607–612 (2010).
25. E. C. Jordan, *Electromagnetic Waves and Radiating Systems*, pp. 130, Prentice Hall, Englewood Cliffs, New Jersey (1968).
26. C. Y. Jen and C. Richter, "Sample thickness measurement with THz-TDS: resolution and implications," *J. Infrared, Millimeter, Terahertz Waves* **35**, 840–859 (2014).

Jin Zhang received her BS and ME degrees in 2008 and 2011, respectively, both from Northeast Normal University. She is currently a staff member in the College of Instrumentation and Electrical Engineering, Jilin University, while pursuing her PhD degree in electrical engineering. Her research interests are mainly focused on THz imaging technologies and nondestructive testing.

Changcheng Shi received his BS and ME degrees in 2004 and 2007, respectively, both from Huazhong University of Science and Technology. He received his PhD degree in biomedical engineering from Clemson University, United States, in 2012. He joined the Research Center for Terahertz Technology, Chongqing Institute of Green and Intelligent Technology, Chinese Academy of Sciences, in 2013. His research interests are the development of novel terahertz imaging technologies for industrial and biomedical applications.

Yuting Ma is a student in the College of Instrumentation and Electrical Engineering, Jilin University, pursuing MS degree in electrical engineering. Her research interests are THz spectral imaging and biological detection.

Xiaohui Han is a student in the College of Instrumentation and Electrical Engineering, Jilin University, pursuing her MS degree in electrical engineering. Her research interests are THz imaging technologies and nondestructive testing.

Wei Li received her BS degree in applied physics from Hubei University of Engineering, China, in 2013. She is currently a student in the Research Center for Terahertz Technology, Chongqing Institute of Green and Intelligent Technology, Chinese Academy of Sciences, pursuing her ME degree in optoelectronic technology and application. Her research interests focus on the applications of THz technology on nondestructive evaluation.

Tianying Chang graduated from Shandong University in 2009 and worked as a joint PhD candidate at the Stevens Institute of Technology (United States) from 2007 to 2008. After graduation, she was a lecturer in Shandong University at Weihai, and then attended the Polytechnic Institute of New York University (United States) as a postdoctoral research associate. Now, she is an associate professor at Jilin University, China, and her research interests are optical fiber sensors, THz systems, and nano-optics.

Dongshan Wei received his PhD degree from the State Key Laboratory of Polymer Physics and Chemistry, China, in 2007. He had a 4-year postdoctoral training in the departments of mechanical engineering and chemistry at Boston University from 2007 to 2011. He became an associate professor in the Research Center for Terahertz Technology, Chongqing Institute of Green and Intelligent Technology, Chinese Academy of Sciences, in 2011. His research interests focus on molecular dynamics simulation by using density functional theory.

Chunlei Du is a professor and director of the Intelligent Manufacturing Technology Research Institute (IMTRI) at Chongqing Institute of Green and Intelligent Technology, Chinese Academy of Sciences. She started her scientific career in the field of micro- and nano-optics. Many micro- and nano-optical devices and instruments have been developed by her research groups. She has been working in the field of micro- and nano-optics and applications for more than two decades.

Hong-Liang Cui is a "National 1000-Plan" Professor in the College of Instrumentation Science and Electrical Engineering, Jilin University. His previous employment includes appointments as professors of applied physics at Stevens Institute of Technology and New York University. His research efforts have been concentrated in the areas of fiber optical communications and sensing, high-frequency electromagnetic wave propagation and interaction with matter, and high-performance computing approaches to the modeling of physical devices and phenomena.